

Cite this: *New J. Chem.*, 2011, **35**, 672–680

www.rsc.org/njc

PAPER

Reaction kinetics and mechanisms of neonicotinoid pesticides with sulfate radicals†

María L. Dell'Arciprete,^a Carlos J. Cobos,^a Daniel O. Mártire,^a Jorge P. Furlong^b and Mónica C. Gonzalez^{*a}

Received (in Montpellier, France) 22nd September 2010, Accepted 22nd November 2010

DOI: 10.1039/c0nj00726a

The reaction kinetics and mechanisms of three neonicotinoid insecticides, imidacloprid (IMD), thiacloprid (THIA) and acetamiprid (ACT) with sulfate radicals were studied by flash-photolysis of peroxodisulfate, $S_2O_8^{2-}$. The absolute rate constants $(3 \pm 1) \times 10^8$, $(1.1 \pm 0.6) \times 10^9$, and $(3 \pm 1) \times 10^9 \text{ M}^{-1} \text{ s}^{-1}$ were determined for IMD, ACT, and THIA, respectively. The reactivity and absorption spectra of the observed organic intermediates are in line with those reported for α -aminoalkyl radicals, and their absorption spectra agree very well with those estimated employing the time-dependent density functional theory with explicit account for bulk solvent effects. The mono- and di-hydroxylated oxidation products of the insecticides were identified as primary degradation products. The proposed reaction mechanism supports an initial charge transfer from the amidine nitrogen of the insecticides to the sulfate radicals. The pyridine moiety of the insecticides remains unaffected even after long irradiation times, until nicotinic acid is formed.

Introduction

Neonicotinoid insecticides are agonists at nicotinic acetylcholine receptors and therefore show selective toxicity for insects over vertebrates.¹ In particular, acetamiprid ((*E*)-*N*-(6-chloro-3-pyridylmethyl)-*N'*-cyano-*N*-methylacetamide, ACT in Scheme 1) and thiacloprid (3-(6-chloro-3-pyridylmethyl)-2-thiazolidinylidene-cyanamide, THIA in Scheme 1) have been demonstrated to be less toxic towards beneficial insects such as honey bees² than the widely employed imidacloprid (1-(6-chloro-3-pyridylmethyl)-2-nitroimino-imidazolidine, IMD in Scheme 1), and therefore, they are increasingly used. Investigations on the degradation of imidacloprid, thiacloprid and acetamiprid mediated by hydroxyl radicals (HO^\bullet) and toxicity evaluation of the primary oxidation products of the insecticides showed that in all cases, the less toxic 6-chloronicotinic acid was found to be the major product at long irradiation times. However, despite the fact that the half life of the insecticides due to their reaction with HO^\bullet radicals in natural aquatic reservoirs may vary between 5 hours and

19 days, the elimination of the insecticide under such conditions might not improve the quality of the contaminated water, as the primary products of degradation showed considerable toxicity to *Vibrio fischeri* assays.³

Destruction of organic compounds contained in waters and soils by peroxodisulfate oxidation is gaining interest as an *in situ* chemical oxidation (ISCO)^{4,5} because peroxodisulfate may be easily activated to yield the highly reactive sulfate radical ions ($SO_4^{\bullet-}$).⁶ Thus, the study of the reactivity of neonicotinoid insecticides with $SO_4^{\bullet-}$ radicals, and the characterization and reactivity of the organic radicals generated are of environmental interest.

Photolysis of $S_2O_8^{2-}$ with excitation wavelengths $\lambda_{exc} < 300 \text{ nm}$, reaction (1), is a clean source of sulfate radical ions with high quantum yields, independent of pH in the range 3–14.⁷ Flash-photolysis of $S_2O_8^{2-}$ is therefore an appropriate method for time-resolved studies yielding information on absolute rate constants and transient generation.



We report here a kinetic and mechanistic study on the reactions of $SO_4^{\bullet-}$ with neonicotinoid insecticides imidacloprid (IMD), thiacloprid (THIA) and acetamiprid (ACT) at pH 3 and 9. *In situ* generation of $SO_4^{\bullet-}$ is performed by flash-photolysis of $S_2O_8^{2-}$ aqueous solutions.

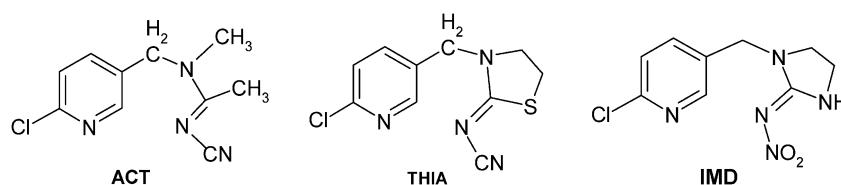
Experimental

Imidacloprid, acetamiprid, and thiacloprid were obtained from Aldrich and used as received. Sodium peroxodisulfate, NaOH, and HClO₄ from Merck were used without further

^a Instituto de Investigaciones Físicoquímicas Teóricas y Aplicadas (INIFTA), Facultad de Ciencias Exactas, Universidad Nacional de La Plata, Casilla de Correo 16, Sucursal 4, (1900) La Plata, Argentina. E-mail: gonzalez@inifta.unlp.edu.ar

^b LADECOR, Departamento de Química, Facultad de Ciencias Exactas, Universidad Nacional de La Plata, Casilla de Correo 16, Sucursal, (1900) La Plata, Argentina

† Electronic supplementary information (ESI) available: The ESI contains details on the kinetic treatment of time-resolved sulfate radicals absorbance profiles, a table with calculated Mulliken atomic charges and a figure showing the TD-DFT calculated spectra of the α -aminoalkyl radicals of ACT protonated in the pyridine ring. See DOI: 10.1039/c0nj00726a



Scheme 1 Chemical structures of the insecticides acetamiprid, thiacloprid, and imidacloprid.

purification. Distilled water was passed through a Millipore system ($> 18 \text{ M}\Omega \text{ cm}^{-1}$, $< 20 \text{ ppb}$ of organic carbon). The pH of the solutions was controlled by addition of either HClO_4 or NaOH as required.

For product detection, aqueous solutions of the pesticides ($2 \times 10^{-4} \text{ M}$) containing $5 \times 10^{-2} \text{ M}$ $\text{Na}_2\text{S}_2\text{O}_8$ solutions were irradiated with 30 flashes of light. Product identification was performed by HPLC-MS analysis (Agilent 1100, equipped with a diode array and ESI/single quadrupole detector). A C18 Restek Pinnacle II column ($250 \text{ mm} \times 2.1 \text{ mm}$ i.d., particle size $5 \mu\text{m}$) was used. The eluent was a mixture of acetonitrile–water 1 : 1 (v/v) at 0.5 mL min^{-1} constant flux. Detection limits were typically 1 ppm. The MS detector was operated in the positive mode with mass detection in the range from 50 to 300 amu. The system used a fragmentation potential of 70 eV. The organic substrates remaining in solution were extracted with a 1 : 1 CH_2Cl_2 –MeOH mixture, the organic phase was separated and evaporated to 1/3 of its volume and further diluted with a 1 : 1 acetonitrile– H_2O mixture. The injection volume was $10 \mu\text{L}$.

Flash-photolysis experiments were carried out using either conventional flash lamps or a laser as the irradiation source. The conventional apparatus was a Xenon Co. model 720C with modified optics and electronics.²⁵ Two collinear quartz Xenon high-intensity pulsed flash tubes, Xenon Corp. P/N 890-1128 (FWHM $\leq 20 \mu\text{s}$), with a continuous spectral distribution ranging from 200 to 600 nm and maximum around 450 nm were used. The analysis source was a high pressure mercury lamp (Osram HBO-100 W). The optical path length of the 1 cm internal diameter quartz sample cell was 10 cm. The monochromator collecting the analysis beam (Bausch & Lomb, high intensity) was directly coupled to a photomultiplier (RCA 1P28), whose output was fed into a digital oscilloscope (HP 54600B). Digital data were stored in a personal computer. The emission of the flash lamps was filtered with an aqueous solution highly concentrated in the corresponding organic compound in order to avoid photolysis of the substrate.

Laser flash photolysis experiments were performed by excitation with the fourth harmonic of a Nd:YAG Litron laser (2 ns FWHM and 6 mJ per pulse at 266 nm). The analysis light from a 150 W Xe arc lamp was passed through a monochromator (PTI 1695) and detected by a 1P28 PTM photomultiplier. Decays typically represented the average of 64 pulses and were taken by and stored in a 500 MHz Agilent Infinium oscilloscope. The photolysis of the substrates was observed to be negligible under the experimental conditions used.

The temperature ($20 \pm 3 \text{ }^\circ\text{C}$) was measured inside the reactor cell with a calibrated Digital Celsius Pt-100 Ω thermometer. Freshly prepared solutions were used in order to avoid

possible thermal reactions of peroxodisulfate with the substrates. Since no important variations in pH (< 0.5 units of pH) were observed after each flash of light or after 64 laser pulses and considering that fresh solutions were used for each experiment, pH may be assumed constant during the irradiation experiments.

Bilinear regression analysis

For each experimental condition, several absorbance decay profiles at different detection wavelengths were taken. Absorbance is thus a function of wavelength and time. A bilinear regression analysis taking advantage of the linearity of the absorbance with both concentrations and absorption coefficients was applied to the experimental absorption matrix in order to retrieve information on the minimum number of species and on their relative concentration profiles and absorption spectra.²⁶

Time-dependent density functional theory calculations

It has been shown that the time-dependent generalization of the density functional theory, TD-DFT, provides remarkable results in the calculation of the observed transition energies of the electronically excited states of a large number of molecules.^{27,28} In particular, the theory gives a well-balanced description for conjugated molecules and open-shell systems such as excited states of radicals.²⁹ In the present study, the hybrid B3LYP density functional was used. This approach implies the Becke's three-parameters exchange functional³⁰ coupled to the nonlocal correlational functional of Lee, Wang, and Parr.³¹ For a more reliable comparison with the experiments, bulk solvent effects were evaluated employing the conductor-like polarizable continuum model, CPCM,³² using for the water a dielectric constant of 78.39. It should be noted that this is a suitable approach as long as no important specific interactions between the solute and solvent molecules are present. All calculations have been performed with the Gaussian 03 package.³³ The absorption spectra were computed following a two-step procedure. Firstly, the optimization of all structural parameters of each ground-state molecule (without symmetry constraints) was performed with the B3LYP/6-311++G(d,p) functional *via* analytic gradient methods. In all the cases, real vibrational frequencies were obtained assuring that molecular structures correspond to energy minima. In the second step, the vertical electronic energies, the associated wavelengths of the band maxima, λ_{max} , and oscillator strengths were computed at the CPCM-B3LYP/6-311++G(d,p) level of theory. The expectation value of the $\langle S^2 \rangle$ operator was not greater than 0.8, close to the exact value of 0.75 for doublet states, therefore indicating

that the spin contamination due to excited states is very small for the investigated intermediates.

The DF-DFT calculations do not account for vibrational broadening. Therefore to compare with experimental results, simulated spectra were obtained by representing each electronic transition with Gaussian shape functions centered at the calculated λ_{\max} . The whole spectra are then obtained considering for all computed transitions a value of $\sigma = 2400 \text{ cm}^{-1}$ for the full width of the band at 1/e height.

Results and discussion

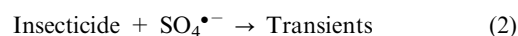
Kinetic measurements

Conventional flash photolysis of air-saturated $5 \times 10^{-2} \text{ M S}_2\text{O}_8^{2-}$ solutions of pH either 3 or 9 showed the formation of a transient species absorbing in the wavelength range from 300 to 600 nm, whose spectrum taken immediately after the flash of light, is in agreement with that reported in the literature for $\text{SO}_4^{\bullet-}$.³ Photolysis of $\text{S}_2\text{O}_8^{2-}$ in the presence of low concentrations ($< 1 \times 10^{-6} \text{ M}$) of the insecticides showed absorption traces at detection wavelengths $\lambda > 350 \text{ nm}$, whose spectrum immediately after the flash of light also agrees with that of $\text{SO}_4^{\bullet-}$ but with faster decay rates (see Fig. 1).

The decay of $\text{SO}_4^{\bullet-}$ absorbance at detection λ , $A(\lambda)$, could be well fitted to eqn (1).

$$A(\lambda) = a(\lambda) \exp(-k_{\text{app}} \times t) + c(\lambda) \quad (1)$$

The small residual absorbance [$c(\lambda)$ in eqn (1)] is associated with long-living species, mainly the organic radicals formed by reaction (2).



The apparent rate constant, k_{app} , is independent of wavelength λ and linearly increases with the analytical concentration of the insecticide, $[\text{Ins}]_0$, as expected from reaction (2) and shown in Fig. 2 for IMD, THIA, and ACT at pH 3 and 9. The slope of these straight lines yields the bimolecular rate constants k_2 , depicted in Table 1. See ESI† for a detailed explanation of the kinetic treatment of time-resolved data.

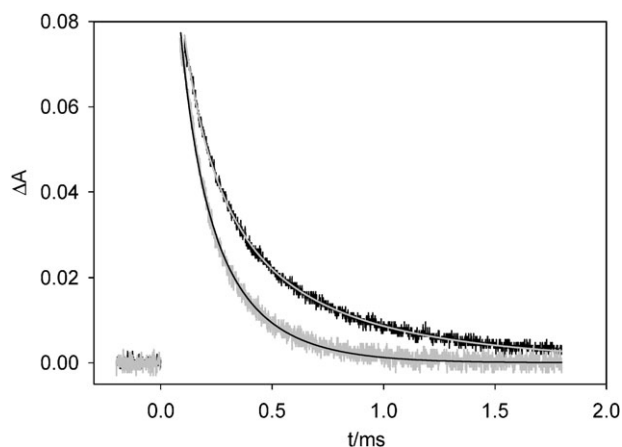


Fig. 1 Absorbance traces at 450 nm obtained in experiments with $5 \times 10^{-2} \text{ M Na}_2\text{S}_2\text{O}_8$ solutions in the presence (grey curve) and absence (black curve) of $1 \times 10^{-6} \text{ M}$ the IMD. The full lines stand for the fittings to eqn (1).

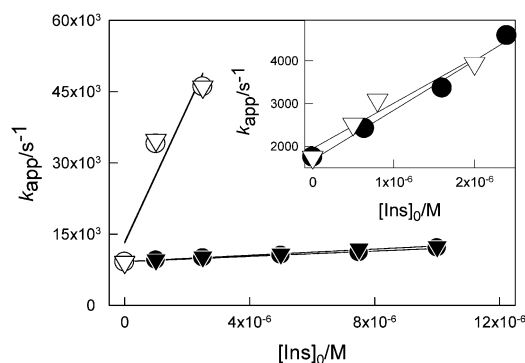


Fig. 2 Apparent rate constants, k_{app} , vs. $[\text{Ins}]_0$ for IMD (black symbols) and THIA (open symbols) obtained in experiments with $5 \times 10^{-3} \text{ M Na}_2\text{S}_2\text{O}_8$ aqueous solutions of pH 3 (circles) and 9 (triangles). Inset: k_{app} vs. $[\text{Ins}]_0$ for ACT obtained in experiments with $5 \times 10^{-3} \text{ M Na}_2\text{S}_2\text{O}_8$ aqueous solutions of pH 3 (circles) and 9 (triangles).

Table 1 Bimolecular rate constants k_2 obtained for IMD, ACT, and THIA at pH 3 and 9

Insecticide	IMD	ACT	THIA
$k_2/\text{M}^{-1} \text{ s}^{-1}$	pH 3 $(3 \pm 1) \times 10^8$ pH 9 $(3.5 \pm 1) \times 10^8$	$(1.1 \pm 0.6) \times 10^9$ $(1.0 \pm 0.8) \times 10^9$	$(3 \pm 1) \times 10^9$ $(4.5 \pm 1) \times 10^9$

The k_2 values are, within the experimental error, independent of pH for the three insecticides. Therefore, either the $\text{p}K_{\text{a}}$ of the insecticides is out of the working pH range, or the $\text{SO}_4^{\bullet-}$ attack on the insecticides is not significantly affected by the acid–base centre.

Stable products identification

Primary stable degradation products of the insecticides were identified in experiments with aqueous solutions containing $2 \times 10^{-4} \text{ M}$ of the insecticides and $5 \times 10^{-2} \text{ M Na}_2\text{S}_2\text{O}_8$ after 30 flashes of light. The intense microsecond pulses of light allowed the generation of a measurable concentration of primary products, minimizing further reactions of these products with sulfate radicals. Table 2 summarizes the mass spectrometry data (MS) observed for the degradation products of the three insecticides. Under stronger oxidation conditions (longer irradiation times), nicotinic acid is observed to be formed in experiments with the three insecticides.

Organic radicals formed after the reactions of $\text{SO}_4^{\bullet-}$ radicals with the insecticides

In order to characterize the organic radicals formed after reaction (2), argon- or air-saturated $5 \times 10^{-3} \text{ M S}_2\text{O}_8^{2-}$ solutions of pH > 7 with concentrations of the insecticides $\geq 1 \times 10^{-5} \text{ M}$ were irradiated with a conventional flash lamp. Under these conditions, the $\text{SO}_4^{\bullet-}$ lifetime is diminished from 60 μs in the absence of insecticides to $< 2 \mu\text{s}$, and the organic intermediates formed after reaction (2) are the main transients detected in conventional flash photolysis experiments.

For each insecticide, several transient decay profiles were taken at different detection wavelengths within the range 300–500 nm. A bilinear regression analysis was applied to

Table 2 Primary degradation products formed after 30 flashes irradiation of air-saturated aqueous solutions containing 2×10^{-4} M of the insecticides and 5×10^{-2} M $\text{Na}_2\text{S}_2\text{O}_8$. HPLC retention times, R_t , and MS mass to charge ratios, m/z , are given, together with assigned products

Insecticide	m/z	R_t/min	Product assignment
IMD	272(271 + H^+)	1.7	<i>N</i> -[1-[(6-Chloro-3-pyridyl)methyl]-4,5-dihydro-5-hydroxyimidazol-2-yl]nitramide, IMD1 in Scheme 3
	288(287 + H^+)	1.6	<i>N</i> -[1-[(6-Chloro-3-pyridyl)methyl]-4,5-dihydro-4,5-dihydroxyimidazol-2-yl]nitramide, IMD3 in Scheme 3
	270(269 + H^+)	2.1	<i>N</i> -[1-[(6-Chloro-3-pyridyl)methyl]-4,5-dihydro-5-oxoimidazol-2,3-yl]nitramide, IMD2 in Scheme 3
THIA	269(268 + H^+)	2.7	3-[(6-Chloro-3-pyridyl)methyl]-4-hydroxy-2-thiazolidinylidenecyanamide, THIA2 in Scheme 4, or 3-[(6-Chloro-3-pyridyl)hydroxymethyl]-2-thiazolidinylidenecyanamide, THIA1 in Scheme 4
ACT	209(208 + H^+)	2.6	<i>N</i> -[(6-Chloro-3-pyridyl) methyl]- <i>N</i> -cyanoacetamide, ACT2 in Scheme 5
	237(236 + H^+)	6.7	<i>N</i> -[(6-Chloro-3-pyridyl) methyl]- <i>N'</i> -cyano- <i>N</i> -formylacetamide, ACT1 in Scheme 5

the absorbance matrix (see Experimental) to obtain information on the minimum number of species. The bilinear analysis shows that the data obtained for the different insecticides may be described by two absorbing species: an organic transient with absorption maxima around 330–350 nm and 440–450 nm, already present 100 μs after the flash of light, which decays to yield stable products with absorption maxima around 300–350 nm. The transient spectra obtained in argon- and air-saturated solutions of pH 7 are shown in Fig. 3–5 for IMD, ACT, and THIA, respectively.

For each insecticide, the absorption spectra of the transients observed in experiments with argon and air-saturated solutions are coincident, as shown in Fig. 3 to 5. However, the decay of the transients strongly depends on the presence of molecular oxygen. The decay follows a second order rate law in argon-saturated solutions (see insets of Fig. 4 and 5 for the transients decay of ACT and THIA, respectively) with rate constant $2k_{\text{rec}}/\epsilon(\lambda)$ (see Table 3), and a pseudofirst order law under air saturation (see inset of Fig. 3 for the transient decay of IMD). Considering that the dissolved molecular oxygen concentration in air-saturated aqueous solutions at 25 °C is

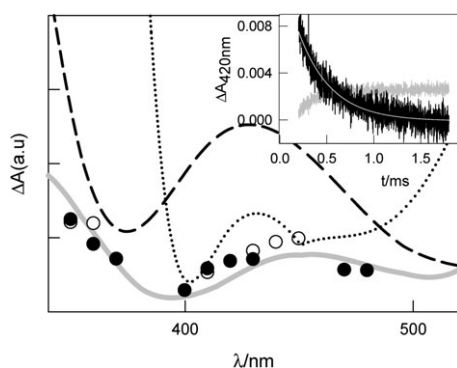


Fig. 3 Absorption spectra (in arbitrary units) of the transients observed in conventional flash-photolysis experiments with: (○) 1×10^{-3} M $\text{S}_2\text{O}_8^{2-}$ and 2×10^{-5} M IMD argon-saturated solutions of pH 7 and (●) 5×10^{-3} M $\text{S}_2\text{O}_8^{2-}$ and 2×10^{-5} M IMD air-saturated solutions of pH 7. The grey line stands for the TD-DFT calculated spectrum for the α -aminoalkyl radical IMDRX (see Scheme 3). The dotted line stands for the calculated absorption spectrum of the α -aminoalkyl radical situated on the methylene bridge, IMDRY, and the dashed line stands for that of the radical cation IMDRC. Inset: transient and stable product (upper and lower traces, respectively) contribution to the absorption traces at 420 nm for experiments with the air-saturated solutions shown in the main figure. The fitting to a first order rate law is overlapped with the experimental curve.

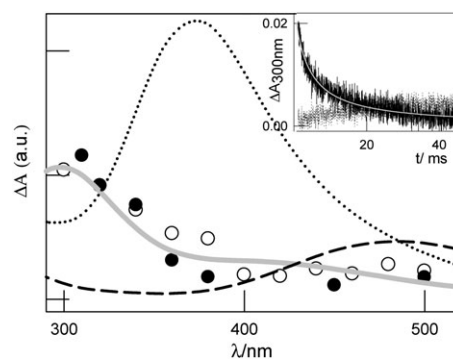


Fig. 4 Absorption spectra (arbitrary units) of the transients observed in conventional flash-photolysis experiments with 5×10^{-3} M $\text{S}_2\text{O}_8^{2-}$ and 1×10^{-5} M ACT in argon- (○) and air-saturated (●) solutions of pH 7. The grey line stands for the TD-DFT calculated spectrum for the α -aminoalkyl radical ACTRX (see Scheme 5). The dotted line stands for the calculated absorption spectrum of the α -aminoalkyl ACTRY and the dashed line stands for that of the radical cation ACTRC. Inset: transient and stable product (upper and lower trace, respectively) contribution to the absorption traces at 300 nm for experiments with the argon-saturated solutions shown in the main figure. The fitting to a second order rate law is overlapped with the experimental curve.

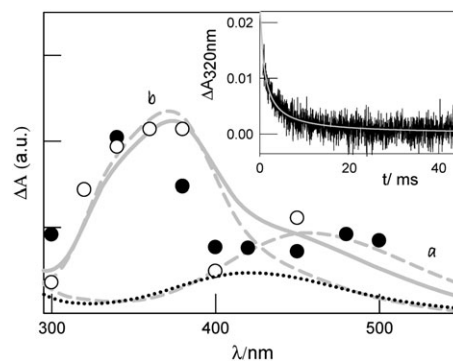


Fig. 5 Absorption spectra (arbitrary units) of the transients observed in conventional flash-photolysis experiments with 5×10^{-3} M $\text{S}_2\text{O}_8^{2-}$ and 1×10^{-5} M THIA in argon- (○) and air-saturated (●) solutions of pH 7. The dashed grey lines stand for the TD-DFT calculated spectrum for the α -aminoalkyl radicals THIARX (curve a) and THIARY (curve b) (see Scheme 2). The grey solid line stands for the linear combination $0.9 \times a + 0.5 \times b$ of curves a and b. The dashed line stands for the calculated absorption spectrum of the radical cation THIARC. Inset: transient contribution to the absorption traces at 320 nm for experiments with the argon-saturated solutions shown in the main figure. The fitting to a second order rate law is overlapped with the experimental curve.

Table 3 Second order decay rate constants $2k_{\text{rec}}/\epsilon$, rate constants for the reaction with molecular oxygen, k_{O_2} , lower limit absorption coefficients, ϵ^{min} , and theoretical values for the absorption coefficient, $\epsilon^{\text{TD-DFT}}$, for the α -aminoalkyl radicals IMDRX, THIARX and THIARY, and ACTRX shown in Schemes 3–5, respectively

Insecticide	IMDRX	ACTRX	THIARX + THIARY ^a
$2k_{\text{rec}}/\epsilon(\lambda)/\text{cm s}^{-1}$	3×10^6 (350 nm)	3×10^5 (300 nm)	5×10^5 (320 nm)
$k_{\text{O}_2}/\text{M}^{-1} \text{s}^{-1}$	1.2×10^7	5×10^5	$(4-6) \times 10^5$
$\epsilon^{\text{min}}(\lambda)/\text{M}^{-1} \text{cm}^{-1}$	1200 (350 nm) 400 (450 nm)	1.2×10^4 (300 nm)	1×10^4 (320 nm)
$\epsilon^{\text{TD-DFT}}(\lambda)/\text{M}^{-1} \text{cm}^{-1}$	700 (350 nm) 380 (450 nm)	1×10^4 (300 nm)	1.45×10^4 (320 nm)

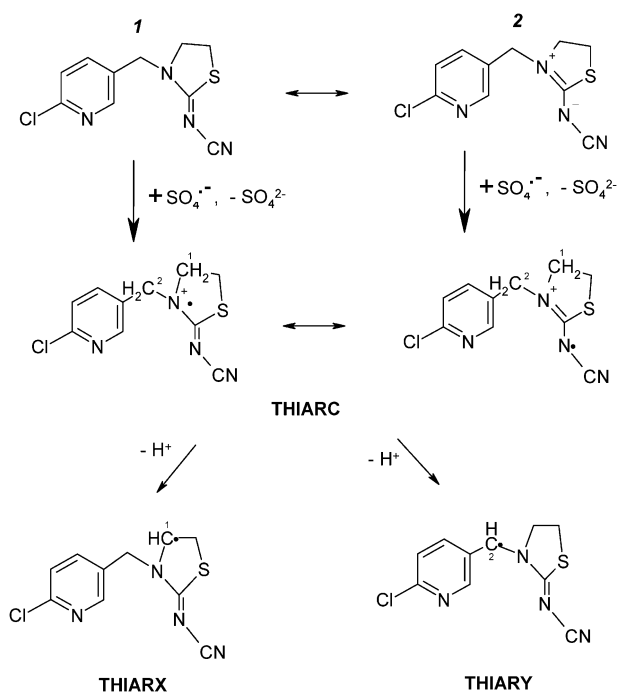
^a Corresponds to a mixture of 0.9 moles of THIA and 0.5 moles of THIARY.

2.5×10^{-4} M, the bimolecular rate constants k_{O_2} for the reaction of the transients with molecular oxygen are obtained (Table 3).

Assuming that the observed transients are the only organic intermediates formed after reaction (2), and considering that $\text{S}_2\text{O}_8^{2-}$ competes with the insecticide for $\text{SO}_4^{\bullet-}$ with reaction rate constant $k_{\text{PS}} \approx 1 \times 10^7 \text{ M}^{-1} \text{ s}^{-1}$, the concentration of the organic transients formed is on the order of the photo-generated $[\text{SO}_4^{\bullet-}]$ times the factor $k_2 \times [\text{Ins}]/(k_2 \times [\text{Ins}] + k_{\text{PS}} \times [\text{S}_2\text{O}_8^{2-}])$. The concentration of $\text{SO}_4^{\bullet-}$ may be calculated from the absorption traces at 450 nm obtained in experiments in the absence of the insecticides, but otherwise identical conditions, taking $\epsilon_{\text{SO}_4^{\bullet-}}(450 \text{ nm}) = 1600 \text{ M}^{-1} \text{ cm}^{-1}$.⁷ From these values and the organic transient absorption extrapolated at time zero, a lower limit for their absorption coefficients, ϵ^{min} , is obtained, as depicted in Table 3. Taking the ϵ^{min} values, the recombination rate constants $2k_{\text{rec}}$ are in the range $(3-5) \times 10^9 \text{ M}^{-1} \text{ s}^{-1}$ for the three insecticides.

Several sites of $\text{SO}_4^{\bullet-}$ attack on the insecticides should be considered. Sulfate radical attack on the pyridine moiety of the insecticides yielding a hydroxylated pyridine ring may be neglected, since neither the observed reaction products, nor the spectra of the observed transients support this reaction pathway.⁷ On the other hand, the rate constants for the sulfate radical H-abstraction from C–H bonds are $(10^5 \text{ to } 10^7 \text{ M}^{-1} \text{ s}^{-1})$ ⁸ much smaller than those measured here for the reactions of $\text{SO}_4^{\bullet-}$ with the insecticides. The one-electron charge transfer reaction from an amine nitrogen to sulfate radicals to yield a radical cation in the N atom has been reported to take place with aliphatic amines,⁹ pyrimidines,¹⁰ cyanuric acid,¹¹ purines,¹² arginine¹³ and tryptophan.¹⁴ Since the three insecticides have amino-type nitrogen atoms in the amidine moiety and the values obtained for k_2 are on the order of those reported for the electron transfer reaction from an unprotonated amine-type nitrogen to the sulfate radicals,⁹ the charge transfer reaction must be considered. Since the one-electron reduction potential for $\text{SO}_4^{\bullet-}$ is $E^\circ(\text{SO}_4^{\bullet-}/\text{SO}_4^{2-}) = 2.5 \text{ V vs. NHE}$ ¹⁵ and the reduction potentials for IMD, ACT, and THIA were reported to be lower than 1.2 V,¹⁶ the variation in the standard free energy for an electron transfer reaction involving the insecticide and the sulfate radicals is thermodynamically allowed, as $\Delta_{\text{ET}}G^0 < -96 \text{ kJ mol}^{-1}$. Scheme 2 shows the proposed reaction including the resonance structures of the amidine group¹⁷ for the insecticide thiacloprid.

Amidines are strong bases ($\text{p}K_{\text{a}} = 6.5-9.6$),¹⁸ whose basicity depends to a great extent on the substituents at the imino-nitrogen



Scheme 2 Mesomeric forms of the amidine group in the insecticide thiacloprid and charge transfer to sulfate as the initial reaction pathway leading to the formation of the radical cation THIARC, followed by H-elimination from the latter to yield α -aminoalkyl radicals THIARX and THIARY.

atom and decreases with the ring size (if they are cyclic as in IMD and THIA) in the sequence $\text{C}_6 > \text{C}_7 > \text{C}_8, \text{C}_5$. The occurrence of the mesomeric form 2 of the imido group (see Scheme 2) supports protonation in the imino nitrogen.¹⁹ Strong electron withdrawing substituents such as NO_2 and CN in the imino nitrogen of IMD and of ACT and THIA, respectively, are expected to considerably diminish the $\text{p}K_{\text{a}}$ of the insecticides. Considering that, within the experimental error, no effect of pH in the range from 3 to 9 was observed on the reaction rate, the $\text{p}K_{\text{a}}$ of the imidine nitrogen in the three insecticides is expected to be < 3 .

Nitrogen-centered radical cations are not prone to efficiently react with molecular oxygen, as observed here for the organic transients.^{7,14} In fact, many literature reports agree in the fact that H atoms in position α to the N atom are easily lost as H^+ to yield an α -aminoalkyl radical highly stabilized by the free electronic pair of the vicinal nitrogen.^{9,10,13} α -Aminoalkyl

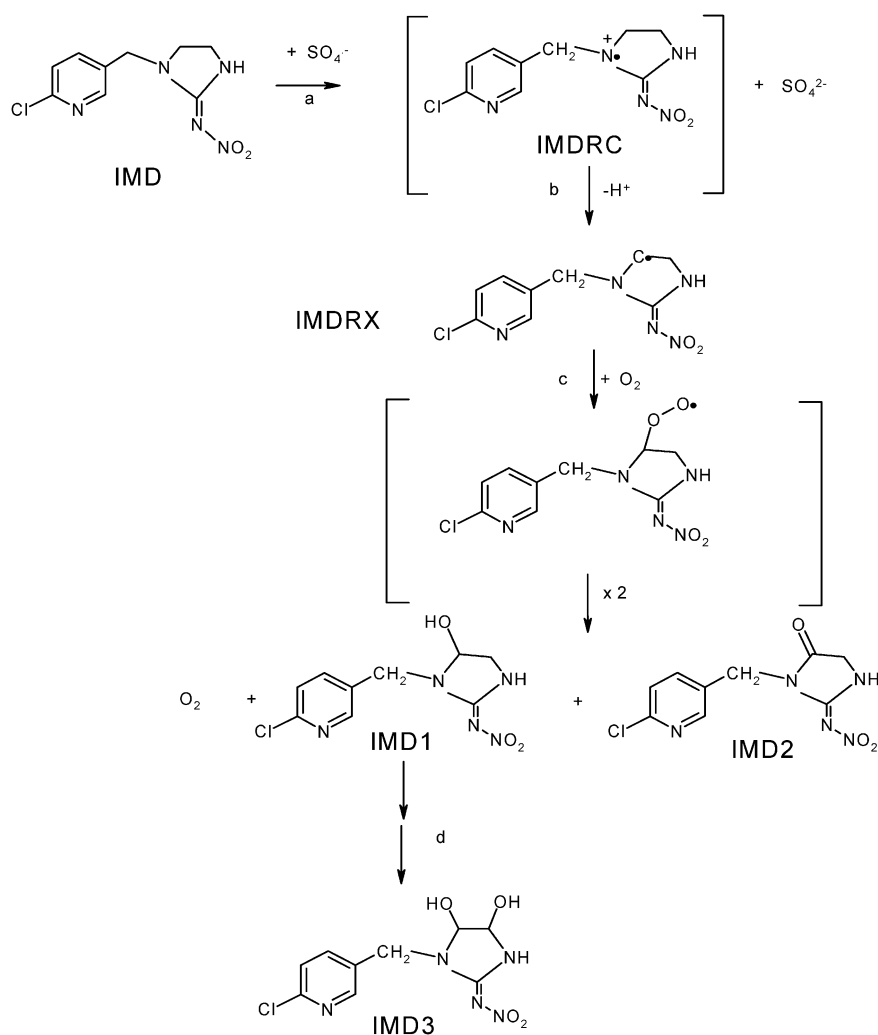
radicals show significant absorbance up to 500 nm and are known to undergo diffusion controlled self-reaction at 298 K in iso-octane solvent²⁰ and to efficiently react with molecular oxygen,^{3,21,22} in agreement with the behavior of the transients herein observed. Therefore, considering that the amine-type nitrogen atom in the amidine moiety of IMD, ACT and THIA, all present H-atoms α to nitrogen, identification of the observed transients as α -aminoalkyl radicals is strongly suggested. Scheme 2 shows the reaction paths leading to the formation of two possible α -aminoalkyl radicals in C1 and C2 of the radical cation.

To help identify the nature of the observed transients, the TD-DFT spectra of α -aminoalkyl radicals in carbon atoms 1 and 2 and the radical cation (now on referred to as RX, RY and RC, respectively) were calculated for each of the insecticides, as also shown for comparison in Fig. 3 to 5. The spectra of the α -aminoalkyl radicals containing the conjugated acid of the pyridine group were also calculated to evaluate the influence of pH on the transient spectra. Interestingly, protonation of the pyridine nitrogen does not significantly affect the radical spectra of the α -aminoalkyl radicals (see ESI†, Fig. S1 for the corresponding spectra for ACT).

The coincidence obtained between the experimental transient spectra and those calculated for the α -aminoalkyl radicals RX, except for THIA, indicates that the observed transients may be assigned to these radicals. The transient spectrum observed for THIA (shown in Fig. 5) can be reproduced from the calculated spectra if 1.8 mol of the α -aminoalkyl radical THIA_{RX} are formed per mol of THIA_{RY}.

The values of ϵ^{min} predicted from the experimental traces of the observed transients and the $\epsilon^{\text{TD-DFT}}$ obtained for the α -aminoalkyl radicals RX from theoretical calculations are, within the error, on the same order of magnitude (see Table 3). Therefore, the α -aminoalkyl radicals IMD_{RX}, ACT_{RX}, THIA_{RX} and THIA_{RY} are the main organic transients detected.

The theoretical calculations show that the difference in energy ΔE between α -aminoalkyl radicals RX and RY is 28.6, 24.8, and 28.6 kJ mole⁻¹ for ACT, THIA and IMD, respectively. Therefore, formation of the α -aminoalkyl radicals RY is expected to be favored. Based on this result, the experimental observation that mainly radicals RX are formed may be a consequence of kinetic limitations precluding the formation of RY. The Mulliken atomic charges in C2 of



Scheme 3 Mechanism for the reaction of IMD with sulfate radical anions. Transients in brackets are proposed, but not detected.

radical cation RC (see Scheme 2) are more negative than in C1 for the three insecticides (see ESI†, Table S1). Therefore, H^+ elimination from C1 in RC is expected to take place more readily than from C2.

The k_{O_2} values reported for several α -aminoalkyl radicals are within the range $(0.04\text{--}3) \times 10^9 \text{ M}^{-1} \text{ s}^{-1}$.²² The k_{O_2} values observed for ACT and THIA are of $5 \times 10^5 \text{ M}^{-1} \text{ s}^{-1}$, therefore suggesting an electron-deficient α -aminoalkyl radical centre in these compounds. It may be expected that a higher delocalization of the unpaired electron in ACT and THIA α -aminoalkyl radicals, compatible with a shift of the absorbance maximum to the visible,^{20,22} further stabilizes the radical diminishing the rate of reaction with molecular oxygen.

Reaction pathways

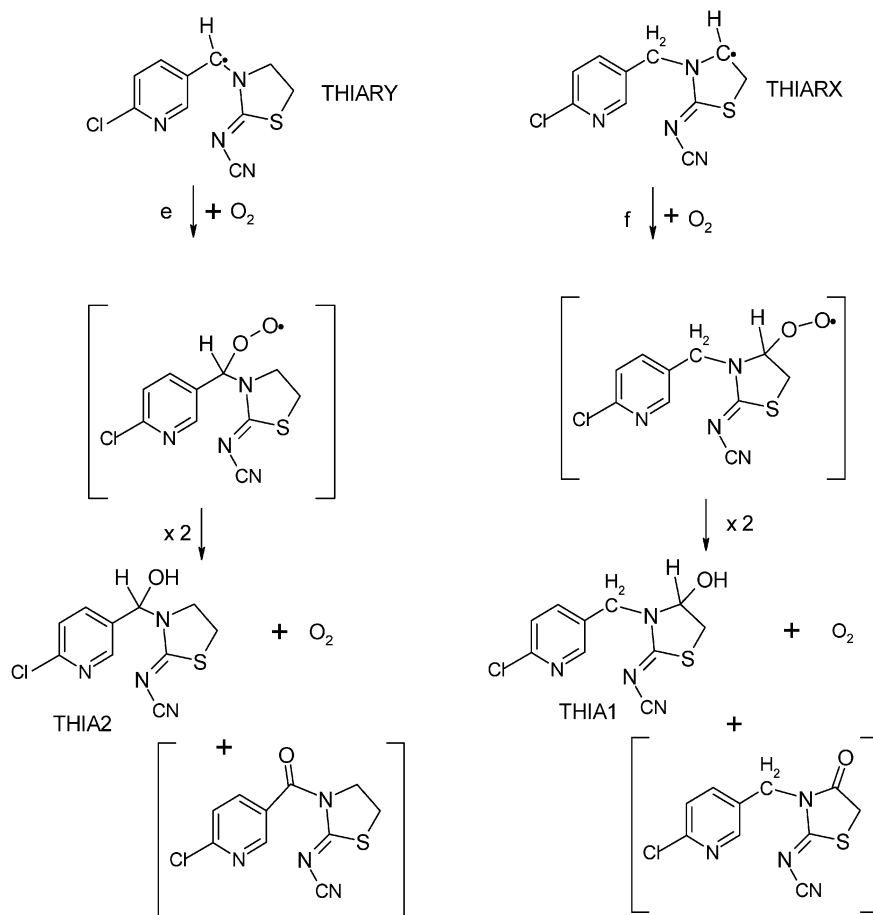
Based on the detected intermediates and the observed reaction products, a pathway for the primary steps of the $SO_4^{\bullet-}$ oxidation of the insecticides may be proposed.

Scheme 3 shows the primary oxidation steps proposed for IMD. As discussed before, a charge transfer pathway leads to the formation of sulfate anions and the radical cation of IMD (reaction path a), which upon elimination of H^+ leads to α -aminoalkyl radical IMDRX (reaction path b). The α -aminoalkyl radicals ($-HC^{\bullet}-N<$) are known by their

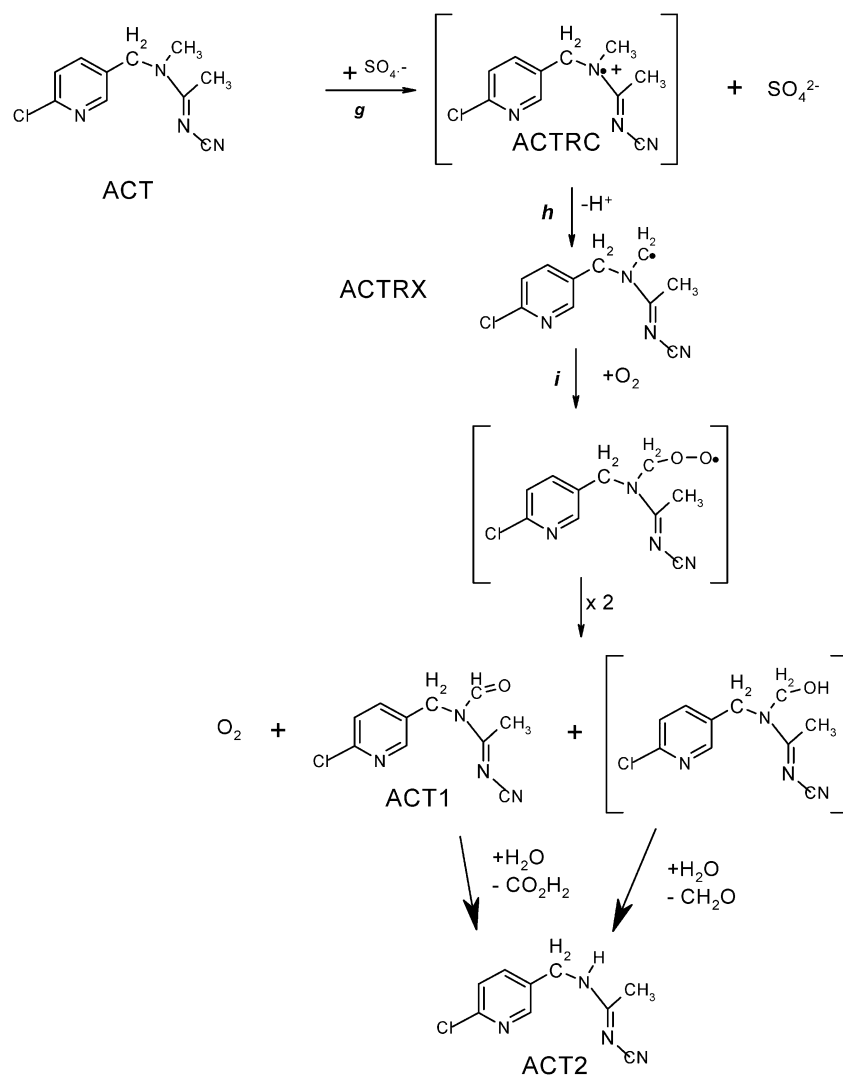
reducing properties^{21,23} and may further react with molecular oxygen to yield peroxide radicals (reaction path c), which upon further disproportionation yield the hydroxyl and keto derivatives of IMD, compounds IMD1 and IMD2, respectively. Further oxidation of compound IMD1 yields the dihydroxylated product IMD3 (reaction path d).

As already discussed, Scheme 2 shows sulfate radical attack to THIA yielding α -aminoalkyl radicals THIA_{RX} and THIA_{RY} with a 1.8 : 1 ratio. Both α -aminoalkyl radicals may further react with molecular oxygen to yield peroxy radicals (reactions paths e and f in Scheme 4), which disproportionate to yield compounds THIA1 and THIA2, and undetected carbonyl derivatives. Despite that only one chromatographic peak was observed, either from compound THIA1 or THIA2, the formation of both compounds cannot be neglected because of the shape of the observed transient spectrum (*vide supra*).

The primary oxidation steps for ACT are shown in Scheme 5. As already proposed for the other insecticides, a charge transfer pathway from the aminic nitrogen in ACT to sulfate radicals yields sulfate anions and the radical cation ACTRC (reaction path g), which upon elimination of H^+ leads to α -aminoalkyl radical ACTRX (reaction path h). Reaction of the latter with molecular oxygen yields peroxy radicals (reaction path i) which disproportionate to the aldehyde (compound ACT1),



Scheme 4 Mechanism for the thermal reactions of the α -aminoalkyl radicals THIA_{RY} and THIA_{RX}. Transients and stable compounds in brackets are proposed, but not detected.



Scheme 5 Mechanism for the reaction of ACT with sulfate radical anions. Transients and stable compounds in brackets are proposed, but not detected.

molecular oxygen, and a hydroxymethylamine (product not detected). Hydrolysis of the latter (and/or of ACT1) yields the demethylated product ACT2 and formaldehyde (and/or formic acid), in agreement with the proposed demethylation mechanism initiated by HO^\bullet radicals.³

The mechanisms proposed for the oxidation of the three insecticides involve peroxy radical formation, which are known to absorb below 300 nm.²⁴ Because the high absorption of the solutions below 300 nm hinders any transient detection at these wavelengths, these radicals could not be detected.

Conclusions

The insecticides IMD, ACT, and THIA chemically react with sulfate radical anions with rate constants of $(3 \pm 1) \times 10^8$, $(1.1 \pm 0.6) \times 10^9$, and $(3 \pm 1) \times 10^9 \text{ M}^{-1} \text{ s}^{-1}$ at pH 3, respectively. The reactions involve a charge transfer from the insecticide to sulfate radicals, characteristic for tertiary amines. Proton elimination from the α carbon to the N atom yields α -aminoalkyl radicals detected as the main transients

formed. The absorption spectra of the latter radicals estimated employing the time-dependent density functional theory with explicit account for bulk solvent effects are in great accordance with those measured experimentally. The amidine nitrogen of the molecule is the preferred site of attack by $\text{SO}_4^{\bullet-}$ radicals in the three insecticides. In fact, the pyridine group is not oxidised until an advanced oxidation stage of the insecticide to 6-chloro-nicotinic acid is attained, in agreement with reported results on the oxidation of the nicotinoid insecticides with hydroxyl radicals.³

The observed primary oxidation products for the insecticides have been reported to retain certain toxicity in *V. fischeri* assays.³ Therefore, detoxification of soils and contaminated waters with peroxodisulfate-based ISCO technologies requires large enough oxidant residence times to assure the elimination of toxic primary oxidation products and improve the quality of the contaminated media.

In this work, theory and experiments played complementary roles, with theory providing a framework within which the empirical results could be interpreted. As a consequence,

a detailed, well supported reaction mechanism for the interaction of sulfate radicals with neonicotinoid insecticides is postulated.

Acknowledgements

This research was supported by Consejo Nacional de Investigaciones Científicas y Técnicas (CONICET) and Agencia Nacional de Promoción Científica y Tecnológica (PICT 2007 # 00308). M.L.D. thanks CONICET for a graduate studentship. M.C.G. and C.J.C. are research members of CONICET. D.O.M. is a research member of Comisión de Investigaciones Científicas de la Provincia de Buenos Aires (CIC), Argentina.

References

- 1 K. Matsuda, S. D. Buckingham, D. Kleier, J. J. Rauh, M. Grauso and D. B. Sattelle, *Trends Pharmacol. Sci.*, 2001, **22**, 573–580.
- 2 T. Iwasa, N. Motoyama and J. T. Ambrose, *Crop Prot.*, 2004, **23**, 371–378.
- 3 M. L. Dell’Arciprete, L. Santos-Juanes, A. Arques Sanz, R. Vicente, A. M. Amat, J. P. Furlong, D. O. Mártire and M. C. Gonzalez, *Photochem. Photobiol. Sci.*, 2009, **8**, 1016–1023.
- 4 (a) C. Liang, C. J. Bruell, M. C. Marley and K. L. Sperry, *Chemosphere*, 2004, **55**, 1225–1233; (b) P. A. Block, R. A. Brown, D. Robinson, Proceedings of the fourth international conference on the remediation of chlorinated and recalcitrant compounds, 2004; (c) K.-C. Huang, Z. Zhao, G. E. Hoag, A. Dahmani and P. A. Block, *Chemosphere*, 2005, **61**, 551–560.
- 5 D. Amarante, *Pollut. Eng.*, 2000, **32**, 40–42.
- 6 V. C. Mora, J. A. Rosso, G. Carrillo Le Roux, D. O. Mártire and M. C. Gonzalez, *Chemosphere*, 2009, **75**, 1405–1409.
- 7 M. L. Dell’Arciprete, C. J. Cobos, J. P. Furlong, D. O. Mártire and M. C. Gonzalez, *ChemPhysChem*, 2007, **8**, 2498–2505.
- 8 P. Neta, R. E. Huie and A. B. Ross, *J. Phys. Chem. Ref. Data*, 1988, **17**, 1027–1284.
- 9 S. Padmaja, Z. Alfassi, P. Neta and R. Huei, *Int. J. Chem. Kinet.*, 1993, **25**, 193–198.
- 10 T. L. Luke, H. Mohan, V. M. Manoj, P. Manoj, J. P. Mittal and C. T. Aravindakumar, *Res. Chem. Intermed.*, 2003, **29**(4), 379–391.
- 11 P. Manoj, R. Varghese, V. M. Manoj and C. T. Aravindakumar, *Chem. Lett.*, 2002, 74.
- 12 A. Vieira, J. Telo, H. Pereira, P. Patrocínio and R. Dias, *J. Chim. Phys. Phys.-Chim. Biol.*, 1999, **96**, 116–123.
- 13 T. Ito, S. Morimoto, S. Fujita and S. Nishimoto, *Radiat. Phys. Chem.*, 2009, **78**, 256–260.
- 14 G. Bosio, S. Criado, W. Massad, M. C. Gonzalez, N. A. García and D. O. Mártire, *Photochem. Photobiol. Sci.*, 2005, **4**, 840–846.
- 15 P. Wardman, *J. Phys. Chem. Ref. Data*, 1989, **18**, 1637–1755.
- 16 M. L. Dell’Arciprete, L. Santos-Juanes, A. Arques, R. F. Vercher, A. M. Amat, J. P. Furlong, D. O. Mártire and M. C. Gonzalez, *Catal. Today*, 2010, **151**, 137–142.
- 17 A. A. Aly and A. M. Nour-El-Din, Special Issue Reviews and Accounts, *ARKIVOC*, 2008, I, 153–194.
- 18 V. G. Granik, *Russ. Chem. Rev. (Engl. Transl.)*, 1983, **52**, 669–703.
- 19 E. Raczynska and J. Oczzapowicz, *Tetrahedron*, 1985, **41**, 5175–5179.
- 20 P. Marriott, R. Castelhan and D. Riller, *Can. J. Chem.*, 1982, **60**, 274–278.
- 21 K. O. Hiller and K. D. Asmus, *J. Phys. Chem.*, 1983, **87**, 3682–3688.
- 22 J. Lalevée, B. Graff, X. Allonas and J. P. Fouassier, *J. Phys. Chem. A*, 2007, **111**, 6991–6998.
- 23 E. Baciocchi, T. Del Giacco and A. Lapi, *Org. Lett.*, 2004, **6**, 4791–4794.
- 24 C. von Sonntag and H. Schuchmann, in *The Chemistry of Free Radicals*, ed. Z. B. Alfassi, Wiley, Chichester, 1997.
- 25 M. L. Alegre, M. Geronés, J. A. Rosso, S. G. Bertolotti, A. M. Braun, D. O. Mártire and M. C. Gonzalez, *J. Phys. Chem. A*, 2000, **104**, 3117–3125.
- 26 E. A. San Román and M. C. Gonzalez, *J. Phys. Chem.*, 1989, **93**, 3532–3536.
- 27 K. B. Wiberg, R. E. Stratman and M. J. Frisch, *Chem. Phys. Lett.*, 1998, **297**, 60–64.
- 28 W. J. McElroy and S. J. Waygood, *J. Chem. Soc., Faraday Trans.*, 1990, **86**, 2557–2564.
- 29 S. Hirata and M. Head-Gordon, *Chem. Phys. Lett.*, 1999, **302**, 375–382.
- 30 A. D. Becke, *Phys. Rev. A: At., Mol., Opt. Phys.*, 1988, **38**, 3098–3100.
- 31 C. Lee, W. Wang and R. G. Parr, *Phys. Rev. B: Condens. Matter*, 1988, **37**, 785–789.
- 32 V. Barone and M. Cossi, *J. Phys. Chem. A*, 1998, **102**, 1995.
- 33 M. J. Frisch, G. W. Trucks, H. B. Schlegel, G. E. Scuseria, M. A. Robb, J. R. Cheeseman, J. A. Montgomery, Jr., T. Vreven, K. N. Kudin, J. C. Burant, J. M. Millam, S. S. Iyengar, J. Tomasi, V. Barone, B. Mennucci, M. Cossi, G. Scalmani, N. Rega, G. A. Petersson, H. Nakatsuji, M. Hada, M. Ehara, K. Toyota, R. Fukuda, J. Hasegawa, M. Ishida, T. Nakajima, Y. Honda, O. Kitao, H. Nakai, M. Klene, X. Li, J. E. Knox, H. P. Hratchian, J. B. Cross, C. Adamo, J. Jaramillo, R. Gomperts, R. E. Stratmann, O. Yazyev, A. J. Austin, R. Cammi, C. Pomelli, J. W. Ochterski, P. Y. Ayala, K. Morokuma, G. A. Voth, P. Salvador, J. J. Dannenberg, V. G. Zakrzewski, S. Dapprich, A. D. Daniels, M. C. Strain, O. Farkas, D. K. Malick, A. D. Rabuck, K. Raghavachari, J. B. Foresman, J. V. Ortiz, Q. Cui, A. G. Baboul, S. Clifford, J. Cioslowski, B. B. Stefanov, G. Liu, A. Liashenko, P. Piskorz, I. Komaromi, R. L. Martin, D. J. Fox, T. Keith, M. A. Al-Laham, C. Y. Peng, A. Nanayakkara, M. Challacombe, P. M. W. Gill, B. Johnson, W. Chen, M. W. Wong, C. Gonzalez and J. A. Pople, *Gaussian 03, Revision C.02*, Gaussian, Inc., Pittsburgh, PA, 2004.